Interacting electrons in one-dimensional quantum rings in a threading magnetic field: Spin phases and correlation

S. Bellucci[1] and P. Onorato[1,2]
[1]*INFN, Laboratori Nazionali di Frascati, P.O. Box 13, 00044 Frascati, Italy*
[2]*Department of Physics "A. Volta," University of Pavia, Via Bassi 6, I-27100 Pavia, Italy*
(Received 22 April 2009; revised manuscript received 27 October 2009; published 24 November 2009)

We study N_e interacting electrons confined in a one-dimensional quantum ring (QR) first by using a Hartree-Fock approximation and then by introducing correlation effects. An external magnetic field B perpendicular to the ring plane is considered. The energy spectra of low-lying states of the QR as a function of B and N_e are obtained. A phase diagram is presented indicating a rich variety of ground states. By plotting the density functions of the QR, the ground-state configuration is found to be a regular polygon.

DOI: 10.1103/PhysRevB.80.195115 PACS number(s): 73.21.−b, 73.23.−b, 73.63.−b

I. INTRODUCTION

In recent years both experimental and theoretical physics communities have devoted a great deal of attention to the nanostuctures and their electronic properties.[1] In particular a big effort has been devoted to the study and the realization of devices with a ring geometry at nanometric scale, known as quantum rings (QRs). A growing interest in studying QRs arises because these systems are known to exhibit many novel physical phenomena, e.g., persistent currents[2–10] and quantum-interference effects (which represent a paradigm of quantum-mechanical phase coherence[11,12]). Among these, the most famous are the magnetic effect [Aharonov-Bohm[13] (AB) effect] or the electric one [Aharonov-Casher[14] (AC) effect for particles with spin].

More recently advances in nanofabrication technology allow for a certain number of electrons to be confined in quantum rings QRs.[15,16] Thus the problem of a few electrons in QRs has been widely investigated[16,17] by focusing both on the transport and optical properties of interacting electrons[18](energy levels and far-infrared spectroscopy[19]). Specifically the energy spectra and the fractional oscillations of the ground state were studied[17,20–22] also by including the effect of the magnetic field.[23–27] Recently the combined effect of the magnetic field and the QR size has been clarified from three up to six electrons by the exact diagonalization approach[28,29] also by focusing on the phase diagram, in the radius versus magnetic field plane, where the spin and angular-momentum transitions are shown.[30]

In this paper we study N_e electrons, interacting by a short-range repulsion, confined in a one-dimensional (1D) QR. First we adopt a Hartree-Fock (HF) approach and then we include some corrections due to correlation effects. In Sec. II we introduce the model and the basic blocks of our calculations.

In Sec. III A we evaluate the many-body energies of the basis functions numerically constructed by a set of single-electron states. The spectrum and eigenfunctions of the QRs are then calculated. The energy spectra of low-lying states of the QR as a function of an external magnetic field B perpendicular to the ring plane are also obtained. Phase diagrams in the U-B (where U is the interaction strength), R-B (where R is the ring radius) and B-N_e are presented indicating a rich variety of ground states.

In Sec. III B we discuss the effects of correlation by including the first higher terms of the perturbative expansion in the interaction. In Sec III C we discuss the basic ground-state configurations by plotting the two-body density functions of some of the many-body states. The latter configurations are found to be regular polygons (RPs).

II. MODEL AND THEORETICAL APPROACHES

Model. Let a N_e-electron planar QR be laid on the x-y plane. A magnetic field B is applied perpendicularly to the plane. The Hamiltonian of the QR reads as

$$H = \left[\sum_i \frac{\left(\mathbf{p_i} - \frac{\mathbf{e}}{\mathbf{c}}\mathbf{A}(\mathbf{r_i})\right)^2}{2m^*}\right] + \left[\sum_{i<j} U(|\mathbf{r_i} - \mathbf{r_j}|)\right]. \quad (1)$$

The first and second parts of Eq. (1) are the single-particle and interaction energies of the electrons, respectively, $\mathbf{A}$ is the vector potential of the magnetic field and m^* is the effective mass.

Single electron. The general form of the single-particle eigenstates is $\phi_m(\mathbf{r}) = e^{im\varphi}$ where m is the orbital angular-momentum quantum numbers and the corresponding single-particle energy is given by

$$\varepsilon_m = \left(m + \frac{\Phi}{\Phi_0}\right)^2 \hbar\omega_R, \quad (2)$$

where $\hbar\omega_R = \frac{\hbar^2}{2m^*R^2}$, Φ is the magnetic flux threading the ring ($\Phi = \pi R^2$), and $\Phi_0 = eh/c$ is the flux quantum. The single-particle energies as a function of the magnetic field are reported in the left panel of Fig. 1, while on the right we show the dispersion relation, $\varepsilon(m)$, and the quantized levels, by focusing on the two symmetries of the shell structure [for integer and half integer values of the $\Phi(B)/\Phi_0$ ratio].

Many-electron ring. We can use the obtained single-particle eigenstates in order to construct the Hamiltonian in Eq. (1) in the Fock space which can be written as

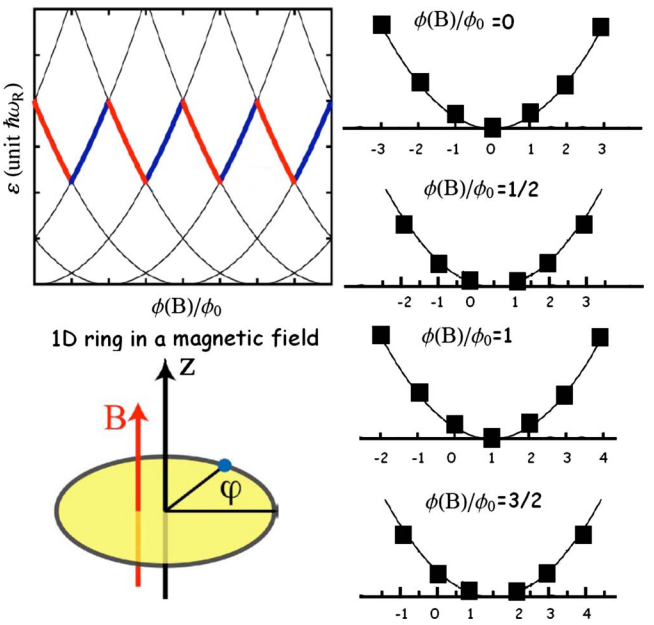

FIG. 1. (Color online) (Left) Single-particle spectrum versus magnetic field. (Right) The dispersion relation and the quantized levels. The boxes in the figure represent energy levels and can be filled by a pair of electrons with opposite spins. In the absence of magnetic field (top) the lowest energy levels correspond to $m=0$, $m=\pm 1$ (degenerate), and so on. When $\Phi(B)=(2n+1)/2\Phi_0$ the lowest degenerate states are given by $m=n$ and $m=n+1$. When $\Phi(B)=n\Phi_0$ the lowest energy state is given by $m=n$.

$$\hat{H}_0 = \sum_{\alpha}^{\infty} \varepsilon_\alpha \hat{n}_\alpha + \frac{1}{2}\sum_{\alpha,\beta,q} V_{\alpha,\beta}(q)\hat{c}^\dagger_{\alpha+q}\hat{c}^\dagger_{\beta-q}\hat{c}_\alpha\hat{c}_\beta, \tag{3}$$

where $\alpha \equiv (m,s)$ denotes the single-particle state, $\hat{c}^\dagger_\alpha$ creates a particle in the state α, $\hat{n}_\alpha \equiv \hat{c}^\dagger_\alpha \hat{c}_\alpha$ is the occupation number operator and $V(q)$ is the Fourier transform of the electron-electron interaction. Because of the symmetries of Eq. (3) due to the properties of electron-electron interaction, once the number of electrons in the QR (N_e) is fixed, we can characterize the ground state (GS) with its spin S and angular momentum M.

Constant interaction (CI) approximation. In some special cases, such as the one of very short-range interaction $U(x)$, we can replace $V_{\alpha,\beta}(q)$ with constant coupling strengths (see the Appendix): $g^\parallel$ (corresponding to a scattering process involving electrons with the same spin) and $g^\perp$ (corresponding to a scattering process involving electrons with opposite spins). Thus Eq. (3) becomes

$$\begin{aligned} H_0^\alpha = {} & \hbar\omega_R \sum_{m,s}\left(m+\frac{\Phi}{\Phi_0}\right)^2 c^\dagger_{m,s}c_{m,s} \\ & + \sum_{m,\mu,q}\sum_{s,\sigma} g^\parallel \delta_{s,\sigma}(c^\dagger_{m+q,s}c^\dagger_{\mu-q,\sigma}c_{m,s}c_{\mu,\sigma}) \\ & + \sum_{m,\mu,q}\sum_{s,\sigma} g^\perp \delta_{s,-\sigma}(c^\dagger_{m+q,s}c^\dagger_{\mu-q,\sigma}c_{m,s}c_{\mu,\sigma}). \end{aligned} \tag{4}$$

Notice that in the QR the interaction parameters, g^i, do not depend on the magnetic field. This yields a relevant difference with respect to the physics of a disk shaped quantum dot.[31,32]

We recall that, when a magnetic field is present, we should take into account also the Zeeman effect. However, because in semiconductors the band effect renormalizes the electron mass, the Zeeman splitting is strongly reduced, while the kinetic energy increases. Thus it was customary to neglect the effects of the Zeeman coupling in typical low dimensional electron systems, such as quantum dots[31,32] or Quantum hall ferromagnets[33] where the spin polarization is essentially based on the effects of the repulsive interaction.

Hartree-Fock approximation. Once the number of electrons N_e has been fixed, we numerically generate many-body states $\Psi_{N_e,M,S,\alpha}$ (α labels different states with the same M and S) and then evaluate the Hartree-Fock many-body spectra by using the methods as outlined in Ref. 32. We obtain an analytical expression for the many-body energies,

$$\begin{aligned} E^{N_e}_{M,S,\alpha}(\Phi) = {} & \hbar\omega_R\left(N_e\frac{\Phi(B)^2}{\phi_0^2} + QM_\alpha - 2M\frac{\Phi(B)}{\phi_0}\right) + g^\perp\frac{N_e^2}{4} \\ & + g^\parallel\frac{N_e(N_e-2)}{4} - (g^\perp - g^\parallel)S^2, \end{aligned} \tag{5}$$

where we introduced $QM_\alpha = \Sigma m^2$ (the sum is on the occupied single-particle states). Thus the kinetic and the interaction energy depend on two parameters, the kinetic one, $\hbar\omega_R$, and the dimensionless interaction one, $U=(g^\perp - g^\parallel)/(\hbar\omega_R)$, respectively.

Higher-order corrections. The Hartree-Fock approximation for one-dimensional correlated electrons can only work to first order in the interaction amplitude. Thus higher order terms have to be included, in order to describe a one-dimensional system of correlated electrons. In general renormalization-group methods are needed for a detailed analysis of 1D interacting electrons.[34] Moreover a perturbative approach which includes just the lowest orders beyond the HF approximation in our case works very well.[35] The restriction to the lowest perturbative terms is justified by the small ratio $g/(\hbar\omega_R)$ that plays the role of g/v_F in the usual Luttinger model.[36]

III. RESULTS

In this paper we consider QRs with a radius between one and a few hundred nanometers which have a longitudinal energy $\hbar\omega_R$ between 1 and 0.05 meV. In this case U can be realistically assumed to take values in the range 0.5–10, whereas the magnetic field corresponding to a threading flux quantum can be easily obtained experimentally. In what follows we limit ourselves to a range of U between 0 and 4 and a magnetic flux, $\Phi(B) \leq \phi_0$. This is the richest region of the phase diagram.

A. Hartree-Fock approximation

Starting from Eq. (5) we can study the evolution of energy levels of low-lying states as a function of B. First we discuss the effects of magnetic field on the dispersion relation [see Figs. 1 and 2(a)]. Next we assume $N_e=4N_p+2$ (N_e

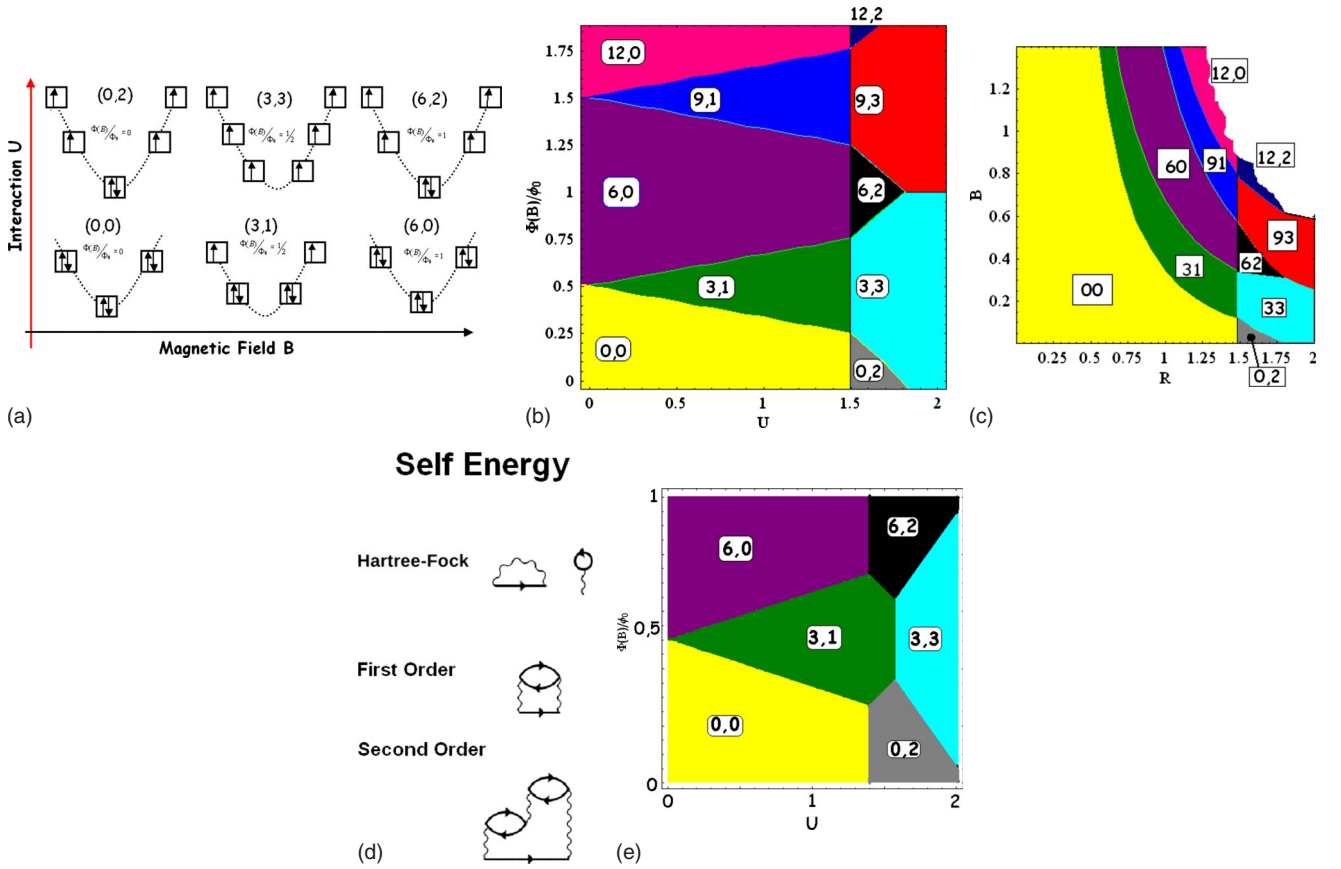

FIG. 2. (Color online) (a) Shells and filling for the main ground states of a six-electron ring as a function of the magnetic field and interaction. (b), (c) The evolution of the ground state as a function of the magnetic field and the electron-electron interaction for a six-electron QR in HF approximation. Angular momenta up to 12 are shown. The numbers inside the figure are (M,S) of each specified domain. Ground states in the U-Φ plane (b) and in the R-B plane (c) [R is given in unit $R_0=\hbar^2/(2m^*U)$ $\omega_R \propto R^{-2}$, $\Phi(B)\propto R^2$, and $U\propto R^{-1}$]. (d) HF contribution to the self energy and first orders bubble contribution included in our calculation. (e) Phase diagram of a six-electron QR obtained including the first orders of perturbation. The effects of correlation are relevant just near the *critical* value of the interaction strength $(U=N_e/4)$.

$=6,10,\ldots$) and present the results first for not interacting electrons, then for interacting ones.

For a noninteracting electron system at vanishing magnetic field all the states below the Fermi level are doubly occupied ($\nu=2$). When a magnetic field corresponding to $\Phi(B)=\Phi_0$ ($\Phi(B)=n\Phi_0$) is present, we have the same dispersion relation of $B=0$, where each electron acquires a quantum, $\hbar$ ($n\hbar$), of the angular momentum. At half field, $\Phi(B)=\Phi_0/2$ ($\Phi(B)=(n+1/2)\Phi_0/2$) there are two electrons in the external shell (consisting of two degenerate states) which is half filled ($1<\nu<2$).

When also the electron-electron interaction is included, some qualitative features can be found as follows:

(i) for a given M state, the energy vs. magnetic field curve is a parabola. This arises from the fact that $E(\Phi)$ in Eq. (5) is a quadratic function of B;

(ii) the increase in B leads to the transitions of the ground state;

(iii) due to these transitions, the energy of the ground state oscillates with increasing B;

(iv) the electron-electron interaction can yield some spin transitions; and

(v) the spin and angular-momentum values of the GS states strongly depend on the strength of U.

The evolution of the ground state (M,S) of the six-electron QR in accordance with B $[\Phi(B)]$ and U (or R) is shown in Fig. 2(b) and 2(c) (for ten electrons in Fig. 3 top, left) where the phase diagram is reported. The numbers inside the figure are (M,S) of each specified domain. The main features of the phase diagram obtained for 6 electrons are stressed as follows:

$(U=0\ R\to\infty)$ M increases in steps of six as B increases, the transitions occur at values of $\Phi=(2n+1)\phi_0/2$, the total spin S is always 0 whereas the lowest single-particle levels are all doubly occupied.

$(0<U<3/2)$ The presence of the interaction allows for the formation of spin polarized ground states at values of the magnetic flux near $\Phi=(2n+1)\phi_0/2$, while at each transition we have $\Delta M=3$ and $|\Delta S|=1$.

$(3/2<U<9/5)$ The presence of the interaction allows for the formation of spin polarized ground states also at values of the magnetic flux near $\Phi=(n)\phi_0[(0,2);(6,2);(12,2)\ldots$, while also in this case at each transition we have $\Delta M=3$ and $|\Delta S|=1$.

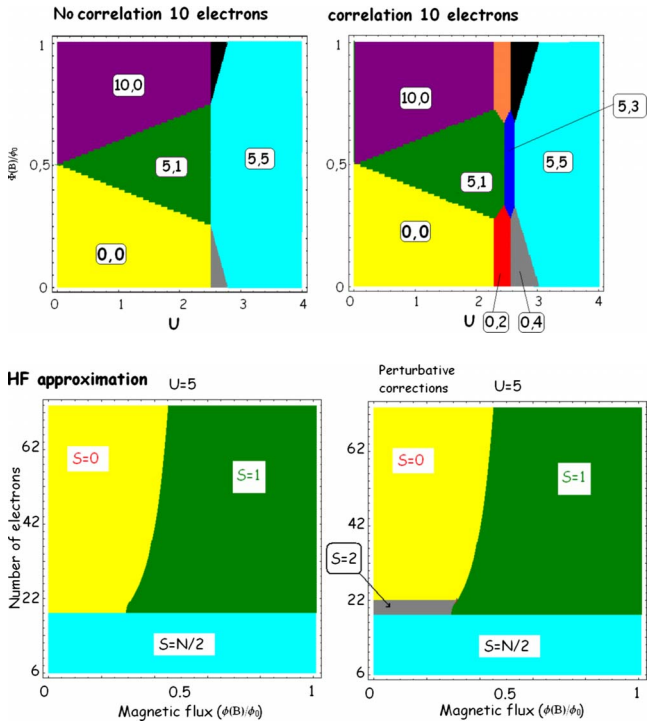

FIG. 3. (Color online) (Top) The evolution of the ground state as a function of magnetic field and electron-electron interaction for a ten-electron QR. Angular momenta up to 10 are shown. Ground State in the U-Φ plane in HF approximation (left) and (right) by including the first perturbative terms. (Bottom) The GS of the many-electron system shown as a function of the number of electrons and the magnetic field. The effects of correlation are evident for low fields near the transition to the spin polarized state.

($U>9/5$) The presence of very strong interaction allows for the formation just of fully spin polarized ground states. In this case at each transition we have $\Delta M=6$ and $|\Delta S|=0$.

The evolution of (M,S) is also reported in the R-B plane in order to allow for a comparison with the results of Ref. 28, where also the Zeeman splitting is included.

By comparing the phase diagrams reported in Fig. 2(b) and the shell filling of the corresponding states reported in Fig. 2(a) we can argue that some symmetric configuration are favored. We can easily generalize the results to the N_e-electron case. At small R (i.e., for $U<N_e/4$) M increases in steps of $N_e/2$ as B increases, while S oscillates between 0 and 1. The increase of M is mainly due to the kinetic term in the Hamiltonian. For $U \gtrsim N_e/4$ M increases in steps of $N_e/2$ as B increases, while S oscillates between $N_e/2-1$ and $N_e/2$. For strong interaction just fully spin polarized ground states, $S=N_e/2$ are allowed while M increases in steps of $N_e/2$, as B increases.

When we analyze the ground-state transition with increasing U for a fixed B and for $N_e=6$, we have three main features: (i) low field: the increasing of interaction allows the formation of spin polarized ground states with transitions $(0,0)\rightarrow(0,2)\rightarrow(3,3)$; (ii) ($\Phi \lesssim \phi_0/2$) the increasing of interaction allows for the formation of spin polarized ground states with transitions $(0,0)\rightarrow(3,1)\rightarrow(3,3)$; and (iii) ($\Phi=\phi_0/2$) the increasing of interaction allows for the formation of spin polarized ground states with a transition $(3,1)\rightarrow(3,3)$.

In general at $U=N_e/4$ a ground-state transition occurs, in which the total spin changes ($S=1\rightarrow N_e/2$ or $S=0\rightarrow N_e/2-1$), while the total angular momentum remains the same. For quite strong interaction (large radius) the fully polarized states ($N_e(k+1/2)$ $N_e/2$ with integer k) dominate.

B. Perturbative terms

Next we can introduce the effects of correlation by taking into account the first perturbative terms beyond the HF approximation (Fig. 2, bottom left). Phase diagrams are presented indicating a rich variety of ground states for six (Fig. 2, bottom right) and ten (Fig. 3, top right) electrons.

When we analyze the ground-state transition with increasing U at a fixed B for $N_e=10$ we have three main features: (i) low field: the increasing of interaction allows for the formation of spin polarized ground states with transitions $(0,0)\rightarrow(0,2)\rightarrow(0,4)\rightarrow(5,5)$; (ii) ($\Phi\sim.3\phi_0$) the increasing of interaction allows for the formation of spin polarized ground states with transitions $(0,0)\rightarrow(5,1)\rightarrow(0,2)\rightarrow(5,3)\rightarrow(0,4)\rightarrow(5,5)$; and (iii) ($\Phi=\phi_0/2$) the increasing of interaction allows for the formation of spin polarized ground states with a transition $\rightarrow(5,1)\rightarrow(5,3)\rightarrow(5,5)$.

In general, when we include perturbative terms, an intermediate phase with even values of the spin is shown near the *critical value* $U=N_e/2$. At some values of the field the electrons flip the spins one by one, while the angular momentum oscillates between the two values ($N_e/2$ and 0). For fields near $\Phi(B)=\Phi_0/2$ the total spin changes with increasing U from $S=1$ to $N_e/2$ two by two when we include perturbative terms.

The effects of correlation are also shown in the diagram in Fig. 3 (bottom), usually reported as a phase diagram, where the spin properties of the Ground State of the many-electron system are shown as a function of the number of electrons and the magnetic field. This diagram can be compared with the analogous one obtained for disk shaped quantum dots (where also the interaction strongly depends on magnetic field). We can argue that the correlation effects can be dominant just near the transition from $S=N/2$ to $S=0$.

C. Ground-state configuration

The effects of the correlation on the many-body wave functions are negligible, unless the strength of the interaction U is $\gtrsim 10^2$. Thus, the GS properties can be explained by the "magic number" theory[37,38] which states that each regular polygon is accessible only to a specific group of states having specific M and S. If N_e electrons in a QR form a N_e-side RP, the potential energy is minimized, hence the total energy is minimized. It is clear that the states reported in the phase diagram fulfill this property. The pursuit of the RP can be demonstrated via the density functions that we introduce following the discussion reported in Ref. 28. So, we define the two-body density functions, $\rho(\varphi_1,\varphi_2)$ and we put the first electron, e_1 at $\varphi_1=0$ location. Thus $\rho(\varphi_2)$ yields the distribution of the second electron e_2, and the maximum of $\rho(\varphi_2)$ is associated with the most probable location of e_2. In our case,

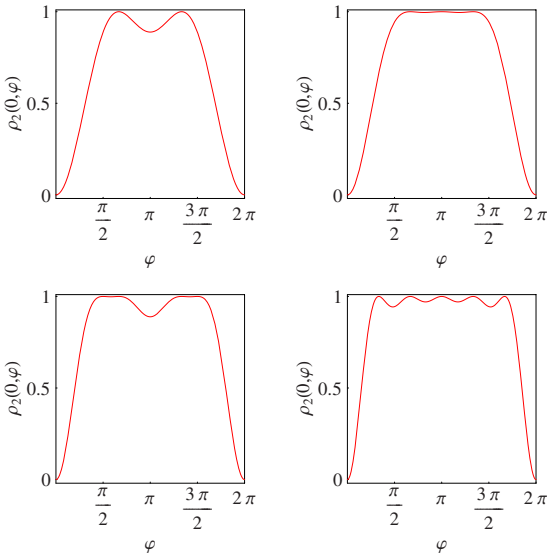

FIG. 4. (Color online) The evolution of ρ_2, for spin polarized up, of the ground state in accordance with φ for a 6 electron ring. The panels correspond to the total spin from 0 to 3 [(0,0),,(3,1),,(0,2), and (3,3)]. The number of up-spin polarized electrons is $N^{\uparrow}=N_e/2+S$, thus the number of peaks in the plots corresponds to $N^{\uparrow}-1$. Each subfigure has $N_{\uparrow}-1$ peaks which are regularly spaced. This fact implies that, if e_1 is fixed at $\varphi=0$, the peaks are the most probable locations of the other up electrons and form electronic configuration with e_1. The most regular configurations correspond to (0,0), (3,1), and (3,3), which yield the main GS also in the corresponding phase diagram.

where correlation is negligible, the pair density can be written in terms of the orbitals of the noninteracting system which is obtained from a Slater determinant.[39] When this definition for the Hartree-Fock pair density is used, it can be shown that the motion of electrons with antiparallel spins is uncorrelated.[40] Some examples of $\rho(\varphi_2)$ of the ground state are plotted in Fig. 4 for $N_e=6$. The most regular configurations correspond to (0,0), (3,1), and (3,3), which yield the main GS also in the corresponding phase diagram.

IV. CONCLUSIONS

In summary, a one-dimensional QR with N_e electrons subjected to an external magnetic field is studied. We obtain the energy spectra of low-lying states of the QR as a function of B for different interaction strength values, U (or different radius values). As a result, the ground state can be determined, and thus the phase diagram, namely, the (M,S) diagram, can be generated. The diagram clearly shows how the ground-state properties vary in accordance with B and U. The physical mechanism of the variation is clarified by focusing on the correlation effects, which yield a rich variety of phases near the critical value of the interaction strength.

Thanks to the HF approximation, we are able to write an analytical expression for the many-body energy, which is useful in order to explain the fundamental mechanism of the spin transition based on the shell structure symmetries. Comparing with the phase diagram obtained in Ref. 28, we find a transition between states in which the total spin changes while the angular momentum remains the same.

The effects of correlation, introduced by taking into account the main perturbative terms, enrich the phase diagrams near the critical points. Thus a varied phase diagram is obtained, owing to correlation effects, by also obtaining the spin flipping one by one (or two by two).

However the perturbative terms do not modify significantly the wave functions of the ground states. This allowed us to show the two-body density functions. In this way, according to earlier papers, it was shown that all ground states were found to possess a RP configuration.[28,29] The ground states which are favored in the phase diagram are those with a regular geometrical configuration, useful in order to minimize the potential energy. Moreover, our approach also enables us to produce a $B-N_e$ phase diagram useful to compare the physics of a QR with that of a disk shaped quantum dot.

From a theoretical point of view, our results can be compared, and are in good agreement, with those obtained for a few to several electrons (between three and six) by the exact diagonalization approach[28,29] (notice that in those calculations also the Zeeman splitting is included). From an experimental point of view, our prediction about the spin and charge transitions could be tested with measurements analogous to those reported in Refs. 31 and 41 for a disk shaped quantum dot. In details, we have in mind a measurement similar to that shown in Fig. 1 of Ref. 41, where the magnetic field evolution of the Coulomb blockade peaks for the first N_e electrons was shown. Moreover a first comparison can be based on the results reported in Fig. (2) of Ref. 16 even though the large width of the QR ($W\sim 250$ nm) analyzed in that experiment introduces some relevant 2D effects (see $\nu>2$ and the presence of spin polarized ($\nu=1$) states also for a small number of electrons.

In this work we considered QRs patterned in a two-dimensional (2D) electron gas at the interface of a semiconductor heterostructure. Thus QRs with a radius between 100 and 500 nm have a longitudinal energy $\hbar\omega_R$ between 1 and 0.05 meV, while a threading flux quantum corresponds to some tens of Tesla, down to a few mT.[42] The electron-electron interaction $g^{\perp}$ can be estimated to range between 2 and 0.5 meV while U can be realistically assumed to be in the range 0.5–10 depending on the width over radius ratio, W/R, which can be assumed to be ~ 0.1 in agreement with Refs. 42 and 43.

APPENDIX: INTERACTION

The interaction parameter can be calculated starting from the Coulomb electron-electron potential[28,29]

$$U(\mathbf{r_i},\mathbf{r_j})=\frac{e^2}{8\pi\varepsilon_0\varepsilon_r\sqrt{d^2+R^2\sin^2[(\theta_i-\theta_j)/2]}}, \qquad \text{(A1)}$$

where d is a small parameter that eliminates the singularity at $(\theta_i-\theta_j)=0$ and gives the effect of finite thickness of the ring, ε_r is the relative static dielectric constant (e.g., 12.4 for GaAs). Thus we can evaluate the interaction parameters,

$$g^{\perp} = \frac{e^2}{8\pi\varepsilon_0\varepsilon_r R}\frac{2K_E(-R^2/d^2)}{d/R},$$

where K_E gives the complete elliptic integral of the first kind, while d/R is assumed as a constructive geometric parameter (d can be estimated as the effective width of the Ring so that even when $g^{\perp}$ shows a logarithmic divergence, the strongest values of the coupling are of order 10). While the $g^{\perp}$ coupling never depends on the states of the interacting electrons in agreement with the CI model, in general $g^{\parallel}$ depends on the relative momenta of the interacting electrons. In the limit of a very short-range interaction $g^{\parallel}=0$ and $g^{\perp}=U$, while for a very long-range interaction $g^{\parallel}=g^{\perp}$ and the electron system can be treated as a noninteracting one. Just in the intermediate regime the CI model can fail, especially for a few-electron ring.

[1] *Mesoscopic Physics and Electronics*, edited by T. Ando, Y. Arakawa, K. Furuya, S. Komiyama, and H. Nakashima (Springer, Berlin, 1998).

[2] M. Büttiker, Y. Imry, and R. Landauer, Phys. Lett. A **96**, 365 (1983).

[3] M. Büttiker, Y. Imry, and M. Ya. Azbel, Phys. Rev. A **30**, 1982 (1984).

[4] H. F. Cheung, Y. Gefen, E. K. Riedel, and W. H. Shih, Phys. Rev. B **37**, 6050 (1988).

[5] D. Loss and P. Goldbart, Phys. Rev. B **43**, 13762 (1991).

[6] H. Bouchiat and G. Montambaux, J. Phys. (France) **50**, 2695 (1989).

[7] G. Montambaux, H. Bouchiat, D. Sigeti, and R. Friesner, Phys. Rev. B **42**, 7647 (1990).

[8] L. P. Lévy, G. Dolan, J. Dunsmuir, and H. Bouchiat, Phys. Rev. Lett. **64**, 2074 (1990).

[9] V. Chandrasekhar, R. A. Webb, M. J. Brady, M. B. Ketchen, W. J. Gallagher, and A. Kleinsasser, Phys. Rev. Lett. **67**, 3578 (1991).

[10] D. Mailly, C. Chapelier, and A. Benoit, Phys. Rev. Lett. **70**, 2020 (1993).

[11] R. A. Webb, S. Washburn, C. P. Umbach, and R. B. Laibowitz, Phys. Rev. Lett. **54**, 2696 (1985).

[12] G. Timp, A. M. Chang, J. E. Cunningham, T. Y. Chang, P. Mankiewich, R. Behringer, and R. E. Howard, Phys. Rev. Lett. **58**, 2814 (1987).

[13] Y. Aharonov and D. Bohm, Phys. Rev. **115**, 485 (1959).

[14] Y. Aharonov and A. Casher, Phys. Rev. Lett. **53**, 319 (1984).

[15] A. Lorke, R. J. Luyken, A. O. Govorov, J. P. Kotthaus, J. M. Garcia, and P. M. Petroff, Phys. Rev. Lett. **84**, 2223 (2000).

[16] U. F. Keyser, C. Fühner, S. Borck, R. J. Haug, M. Bichler, G. Abstreiter, and W. Wegscheider, Phys. Rev. Lett. **90**, 196601 (2003).

[17] Y. Saiga, D. S. Hirashima, and J. Usukura, Phys. Rev. B **75**, 045343 (2007).

[18] L. Wendler, V. M. Fomin, A. V. Chaplik, and A. O. Govorov, Phys. Rev. B **54**, 4794 (1996).

[19] H. Hu, J. L. Zhu, and J. J. Xiong, Phys. Rev. B **62**, 16777 (2000).

[20] A. Emperador, F. Pederiva, and E. Lipparini, Phys. Rev. B **68**, 115312 (2003).

[21] C. G. Bao, G. M. Huang, and Y. M. Liu, Phys. Rev. B **72**, 195310 (2005).

[22] J. L. Zhu, S. Hu, Z. S. Dai, and X. Hu, Phys. Rev. B **72**, 075411 (2005).

[23] Z. Barticevic, M. Pacheco, and A. Latgé, Phys. Rev. B **62**, 6963 (2000).

[24] J. Song and S. E. Ulloa, Phys. Rev. B **63**, 125302 (2001).

[25] J. Planelles, W. Jaskólski, and J. I. Aliaga, Phys. Rev. B **65**, 033306 (2001).

[26] J. B. Xia and S. S. Li, Phys. Rev. B **66**, 035311 (2002).

[27] M. Aichinger, S. A. Chin, E. Krotscheck, and E. Rasanen, Phys. Rev. B **73**, 195310 (2006).

[28] Y. M. Liu, G. M. Huang, and T. Y. Shi, Phys. Rev. B **77**, 115311 (2008).

[29] Y. M. Liu, C. G. Bao, and T. Y. Shi, Phys. Rev. B **73**, 113313 (2006).

[30] N. Yang, Z. Dai, and Jia-Lin Zhu, Phys. Rev. B **77**, 245321 (2008).

[31] O. Klein, C. de C. Chamon, D. Goldhaber-Gordon, M. A. Kastner, and X.-G. Wen, *Phase Transitions in Artificial Atoms*, in Proceedings of the NATO Advanced Study Institute on Quantum Transport in Semiconductor Submicron Structures, NATO ASI Series E, edited by B. Kramer (1996), pp. 239–249; O. Klein, D. Goldhaber-Gordon, C. de C. Chamon, and M. A. Kastner, Phys. Rev. B **53**, R4221 (1996).

[32] S. Bellucci and P. Onorato, Phys. Rev. B **72**, 045345 (2005).

[33] Z. F. Ezawa and G. Tsitsishvili, Rep. Prog. Phys. **72**, 086502 (2009).

[34] S. Bellucci, J. Gonzalez, and P. Onorato, Nucl. Phys. B **663**, 605 (2003); Phys. Rev. B **69**, 085404 (2004); S. Bellucci and P. Onorato, Eur. Phys. J. B **45**, 87 (2005).

[35] A comparison between the perturbative theory and the RG approach to the Luttinger Liquid can be based on the perturbative calculation of the momentum distribution n_k. The results are in good agreement with the ones reported in P.-A. Bares and X. G. Wen, Phys. Rev. B **48**, 8636 (1993).

[36] For a review see J. Solyom, Adv. Phys. **28**, 201 (1979); J. Voit, Rep. Prog. Phys. **57**, 977 (1994); H. Schulz, *Proceedings of Les Houches Summer School LXI*, edited by E. Akkermans, G. Montambaux, J. Pichard, and J. Zinn-Justin (Elsevier, Amsterdam, 1995), p. 533, arXiv:cond-mat/9503150.

[37] W. Y. Ruan, Y. Y. Liu, C. G. Bao, and Z. Q. Zhang, Phys. Rev. B **51**, 7942 (1995).

[38] C. G. Bao, Phys. Rev. Lett. **79**, 3475 (1997).

[39] B. Hetenyi and A. W. Hauser, Phys. Rev. B **77**, 155110 (2008).

[40] A. Szabo and N. Ostlund, *Modern Quantum Chemistry*, 1st ed. (Dover, New York, 1996).

[41] T. H. Oosterkamp, J. W. Janssen, L. P. Kouwenhoven, D. G. Austing, T. Honda, and S. Tarucha, Phys. Rev. Lett. **82**, 2931 (1999).

[42] A. Bruno-Alfonso and A. Latge, Phys. Rev. B **77**, 205303 (2008).

[43] F. Carillo, G. Biasiol, D. Frustaglia, F. Giazotto, L. Sorba, and F. Beltram, Physica E **32**, 53 (2006).